ORIGINAL ARTICLE

Augmented Lipocalin-2 Is Associated with Chronic Obstructive Pulmonary Disease and Counteracts Lung Adenocarcinoma Development

Warapen Treekitkarnmongkol[1]*, Maya Hassane[2]*, Ansam Sinjab[1], Kyle Chang[3], Kieko Hara[1], Zahraa Rahal[4], Jiexin Zhang[5], Wei Lu[1], Smruthy Sivakumar[3], Tina L. McDowell[1,3], Jacob Kantrowitz[6], Jianling Zhou[1], Wenhua Lang[1], Li Xu[1], Joshua K. Ochieng[1], Sayuri Nunomura-Nakamura[7], Shanshan Deng[8], Carmen Behrens[1], Maria Gabriela Raso[1], Junya Fukuoka[7], Alexandre Reuben[9], Edwin J. Ostrin[10], Edwin Parra[1], Luisa M. Solis[1], Avrum E. Spira[6], Florencia McAllister[11], Tina Cascone[9], Ignacio I. Wistuba[1], Seyed Javad Moghaddam[8], Paul A. Scheet[3], Junya Fujimoto[1], and Humam Kadara[1]

[1]Department of Translational Molecular Pathology, [3]Department of Epidemiology, [5]Department of Bioinformatics and Computer Biology, [8]Department of Pulmonary Medicine, [9]Department of Thoracic Head and Neck Medical Oncology, [10]Department of General Internal Medicine, and [11]Department of Clinical Cancer Prevention, The University of Texas MD Anderson Cancer Center, Houston, Texas; [2]Department of Biochemistry and Molecular Genetics and [4]Faculty of Medicine, American University of Beirut, Beirut, Lebanon; [6]Section of Computational Biomedicine, School of Medicine, Boston University, Boston, Massachusetts; and [7]Graduate School of Biomedical Sciences, Nagasaki University, Nagasaki, Japan

Abstract

Rationale: Early pathogenesis of lung adenocarcinoma (LUAD) remains largely unknown. We found that, relative to wild-type littermates, the innate immunomodulator *Lcn2* (lipocalin-2) was increased in normal airways from mice with knockout of the airway lineage gene *Gprc5a* (*Gprc5a*$^{-/-}$) and that are prone to developing inflammation and LUAD. Yet, the role of LCN2 in lung inflammation and LUAD is poorly understood.

Objectives: Delineate the role of *Lcn2* induction in LUAD pathogenesis.

Methods: Normal airway brushings, uninvolved lung tissues, and tumors from *Gprc5a*$^{-/-}$ mice before and after tobacco carcinogen exposure were analyzed by RNA sequencing. *LCN2* mRNA was analyzed in public and in-house data sets of LUAD, lung squamous cancer (LUSC), chronic obstructive pulmonary disease (COPD), and LUAD/LUSC with COPD. LCN2 protein was immunohistochemically analyzed in a tissue microarray of 510 tumors. Temporal lung tumor development, gene expression programs, and host immune responses were compared between *Gprc5a*$^{-/-}$ and *Gprc5a*$^{-/-}$/*Lcn2*$^{-/-}$ littermates.

Measurements and Main Results: *Lcn2* was progressively elevated during LUAD development and positively correlated with proinflammatory cytokines and inflammation gene sets. *LCN2* was distinctively elevated in human LUADs, but not in LUSCs, relative to normal lungs and was associated with COPD among smokers and patients with LUAD. Relative to *Gprc5a*$^{-/-}$ mice, *Gprc5a*$^{-/-}$/*Lcn2*$^{-/-}$ littermates exhibited significantly increased lung tumor development concomitant with reduced T-cell abundance (CD4^{+}) and richness, attenuated antitumor immune gene programs, and increased immune cell expression of protumor inflammatory cytokines.

Conclusions: Augmented LCN2 expression is a molecular feature of COPD-associated LUAD and counteracts LUAD development *in vivo* by maintaining antitumor immunity.

Keywords: lung neoplasms; chronic obstructive pulmonary disease; immunity; lipocalin-2

(Received in original form April 13, 2020; accepted in final form July 30, 2020)

*These authors contributed equally to this work as co–first authors.

Supported in part by National Cancer Institute grant R01CA205608 (H.K.), American Lung Association Lung Cancer Discovery Award (H.K.), University Cancer Foundation Institutional Research Grant (H.K.), and a Medical Practice Plan grant from American University of Beirut (H.K.).

Correspondence and requests for reprints should be addressed to Humam Kadara, Ph.D., Department of Translational Molecular Pathology, The University of Texas MD Anderson Cancer Center, Houston, TX 77030. E-mail: hkadara@mdanderson.org.

This article has a related editorial.

This article has an online supplement, which is accessible from this issue's table of contents at www.atsjournals.org.

Am J Respir Crit Care Med Vol 203, Iss 1, pp 90–101, Jan 1, 2021

Originally Published in Press as DOI: 10.1164/rccm.202004-1079OC on July 30, 2020
Internet address: www.atsjournals.org

At a Glance Commentary

Scientific Knowledge on the Subject: Inflammation in pathological conditions such as chronic obstructive pulmonary disease (COPD) reprograms the immune microenvironment and predisposes tissues to cancer development and progression.

What This Study Adds to the Field: Augmented LCN2 expression is a molecular feature of COPD-associated lung adenocarcinoma and counteracts lung adenocarcinoma development *in vivo* by maintaining antitumor immunity.

Lung adenocarcinoma (LUAD) represents the most common subtype of lung cancer in smokers and accounts for most cancer deaths related to smoking (1). LUAD is typified by poor clinical outcome (1). Despite recent advances in immunotherapy, LUAD displays variable responses to immune-based treatment (2). There are few strategies for prevention or early treatment of LUAD largely because of a paucity of characterized targets in its molecular pathogenesis (3).

Inflammation in pathological conditions such as chronic obstructive pulmonary disease (COPD) reprograms the immune microenvironment and predisposes tissues to cancer development and progression (4, 5). Proinflammatory cytokines such as IL-17A, IL-1β, and IL-6 promote tumor progression, and targeting these cytokines limits lung cancer development (6–8). Treatment with the IL-1β antibody canakinumab was shown to reduce incident lung cancers (6). Airway epithelial cells elicit host defense cues mediated by surfactants, lipocalins, defensins, and antimicrobial proteins to counteract pathogenic effects of inflammation or infection (9, 10). The intricate balance between host defense mechanisms and inflammation, for instance in response to carcinogenic exposures, is thought to be sentinel in disease (9, 11). Yet, for LUAD that is etiologically related to tobacco carcinogen exposure, we poorly understand the role of the earliest host defense and immunomodulatory cues in its development.

We previously showed that mice with knockout of the airway lineage gene *Gprc5a* (G protein-coupled receptor family C type 5A) (*Gprc5a*$^{-/-}$) and exposure to tobacco carcinogen develop, in contrast to wild-type (WT) mice, lung tumors with somatic driver *Kras* variants (12, 13). Here, we found that the lipocalin *Lcn2* was prominently progressively increased early during *in vivo* LUAD development. LCN2 was also distinctively augmented in human LUAD and was strongly associated with COPD among both lung cancer–free smokers and patients with LUAD. Deletion of *Lcn2* in *Gprc5a*$^{-/-}$ mice increased LUAD development as well as elevated protumor inflammatory signaling and reduced antitumor immunity. Our findings suggest that elevated LCN2 is a molecular feature of COPD and antagonizes LUAD development.

Some of the results of this study have been previously reported in the form of an abstract (14).

Methods

Animal Housing and Tobacco Carcinogen Exposure Experiments

Animal experiments were conducted according to Institutional Animal Care and Use Committee–approved protocols. Mice were maintained in a pathogen-free animal facility. *Gprc5a*$^{-/-}$ mice were generated as previously described (12, 13) and crossed with *Lcn2*$^{-/-}$ animals (15) to generate *Gprc5a*$^{-/-}$/*Lcn2*$^{-/-}$ littermates. Sex- and age-matched *Gprc5a*$^{-/-}$ and *Gprc5a*$^{-/-}$/*Lcn2*$^{-/-}$ mice were divided into starting groups of 8–10 mice for assessment at different time points and were intraperitoneally injected with 50 mg/kg of body weight nicotine-specific nitrosamine ketone (NNK) (in phosphate-buffered saline; Toronto Research Chemicals) three times per week for 8 weeks. Lung sections from all mice were analyzed for lung tumor incidence according to previously reported criteria that include assessment of tumor differentiation and invasiveness as well as nuclear crowding, size, and atypia (16). Immunohistochemical assessment of murine LCN2 protein was performed as previously described (15).

Immunohistochemical Analysis of LCN2 and CD4$^+$ T-Cell Densities

Archived surgically resected tumor specimens were collected from patients with non–small cell lung cancer ($n = 510$) evaluated at MD Anderson Cancer Center, and consents were approved by the institution's review board. LCN2 protein was analyzed by immunohistochemistry using a Leica Bond Max automated stainer (Leica Biosystems). After antigen retrieval at 100°C for 20 minutes (Bond ER Solution #1; Leica Biosystems), 4-μm tissue sections were incubated with anti-LCN2 polyclonal goat primary antibody (AF1757, 1:1000 dilution; R&D Systems) and detected using the Bond Polymer Refine Detection kit (DS9800; Leica Biosystems). Cytoplasmic expression of LCN2 was quantified using a four-value staining intensity score (0, none; 1, weak; 2, moderate; and 3, strong) and the extent of reactivity (0–100%). A final expression score (H-score) was obtained by multiplying the intensity and reactivity extension values (range, 0–300) as previously described (17). Preoperatively untreated early-stage (stages 1–3) LUADs with positive LCN2 H-scores (>3) were retained for all analyses ($n = 271$). Immunohistochemical analysis of tumor-infiltrating CD4$^+$ T cells was performed as described previously (18). COPD was assessed based on the guidelines by the Global Initiative for Chronic Obstructive Lung Disease classification—a patient with a postbronchodilation FEV_1/FVC ratio <0.7 was considered as having COPD (19).

Statistical Analysis

All statistical analyses were parametric and performed using GraphPad Prism software

Author Contributions: W.T., M.H., J. Fujimoto, and H.K. conceived the work. W.T., M.H., A.S., Z.R., W. Lang, J.K.O., and S.N.-N. performed animal experiments. W.T., M.H., A.S., K.C., K.H., Z.R., J. Zhang, W. Lu, S.S., T.L.M., J.K., J. Zhou, L.X., S.D., C.B., M.G.R., A.R., E.P., L.M.S., A.E.S., F.M., T.C., S.J.M., P.A.S., J. Fujimoto, and H.K. performed analysis. W.T., M.H., K.C., J. Zhang, S.S., T.L.M., J.K., L.X., A.E.S., T.C., P.A.S., and H.K. performed RNA sequencing and expression profiling analysis. W.T., K.H., W. Lu, J. Zhou, C.B., M.G.R., J. Fukuoka, A.R., L.M.S, I.I.W., S.J.M., J. Fujimoto, and H.K. performed pathology and clinical analyses. E.J.O., A.E.S., F.M., T.C., S.J.M., and P.A.S. provided intellectual input. W.T., M.H., A.S., K.C., K.H., T.L.M., J. Fukuoka, and H.K. wrote the draft of the manuscript. All authors approved the final version of the manuscript. H.K. supervised the study.

and in R (r-project.org). All statistical analyses between two groups were performed using unpaired Student's *t* tests. Correlations between continuous variables were statistically interrogated using Pearson correlation coefficients. Differences among three or more groups were statistically evaluated using ANOVA. Results with *P* values less than 0.05 were considered significant.

Additional details and methods are found in the Supplementary Methods in the online supplement.

Results

Increased *Lcn2* Expression during Early Pathogenesis of LUAD

We previously found that *Gprc5a*$^{-/-}$ mice develop lung tumors with somatic driver mutations in *Kras* (12, 13). We performed RNA sequencing (RNA-seq) analysis of normal airways from 8-week-old *Gprc5a*$^{-/-}$ and WT littermates ($n = 6$ each). We identified 155 gene transcripts that were significantly modulated between *Gprc5a*$^{-/-}$ and WT airways (Table E1 in the online supplement), among which *Lcn2* was distinctively markedly elevated in normal airways from *Gprc5a*$^{-/-}$ mice ($P < 0.05$; Figures 1A and 1B). We then probed *Lcn2* induction in LUAD development. We found that *Lcn2* was significantly and progressively increased with time in normal-appearing airways from *Gprc5a*$^{-/-}$ mice ($n = 6$ mice per time point; all $P < 0.05$; Figure 1C). Not only was *Lcn2* expression consistently elevated in lung tumors ($n = 4$–20 lesions per mouse) compared with matched uninvolved normal tissues ($n = 9$–10 mice per time point) across all time points (all $P < 0.01$), it was also progressively elevated with time in the normal tissues (all $P < 0.01$; Figure 1D). LCN2 protein in BAL fluid was also significantly and progressively increased with time during lung tumorigenesis (all $P < 0.05$; Figure 1E). LCN2 protein was also expressed in epithelial cells from premalignant lesions (hyperplasias and adenomas) and more notably from LUADs (Figure 1F). These findings demonstrate that the innate immunomodulator *Lcn2* is increased early during LUAD pathogenesis.

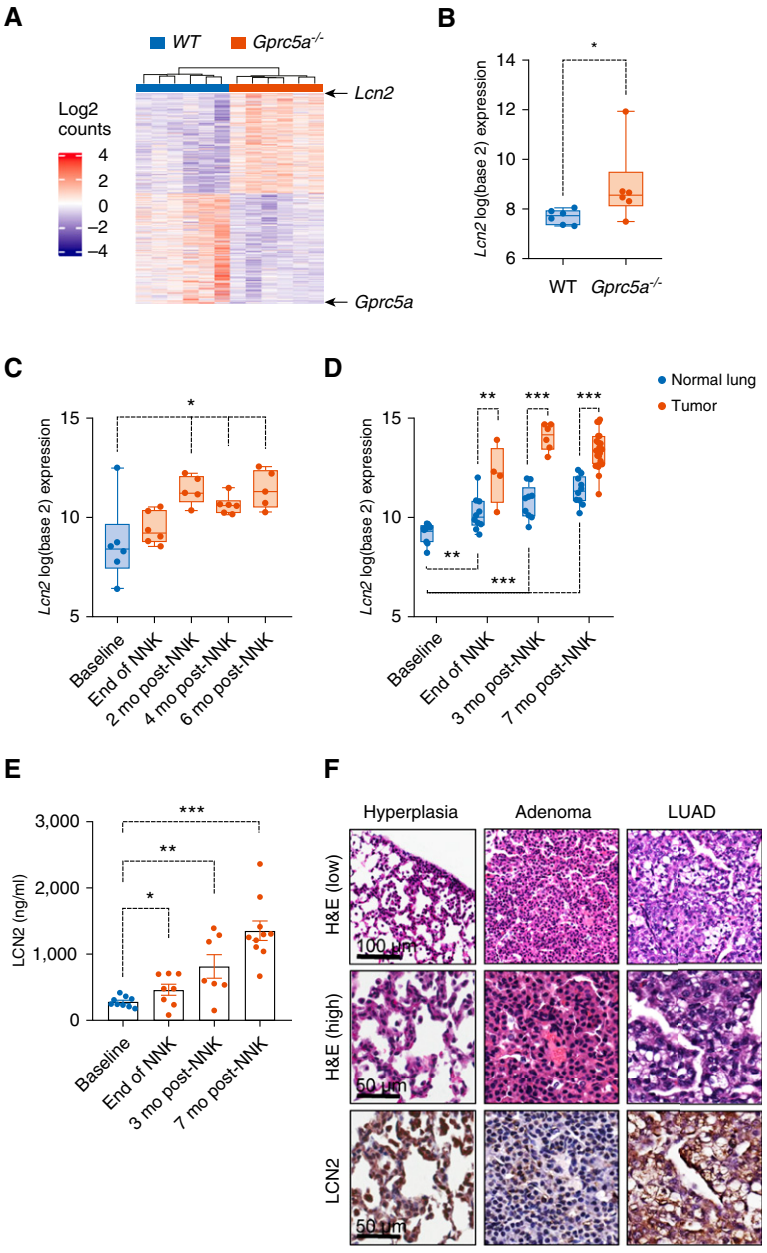

Figure 1. Increased *Lcn2* during lung adenocarcinoma (LUAD) development in *Gprc5a*$^{-/-}$ mice. (*A*) Heat map showing differentially expressed transcripts between normal airways of wild-type (WT) and *Gprc5a*$^{-/-}$ mice ($n = 6$ per genotype) by RNA sequencing (RNA-seq). Columns indicate individual mouse airways and rows indicate transcripts (red, upregulated; blue, downregulated). (*B*) Comparison of *Lcn2* mRNA expression in normal airways between WT (blue) and *Gprc5a*$^{-/-}$ (red) mice. (*C*) Temporal assessment of *Lcn2* mRNA levels by RNA-seq in normal airways of *Gprc5a*$^{-/-}$ mice ($n = 6$ per time point) before treatment (baseline) and at various time points after NNK exposure (end of NNK and 2, 4, and 6 mo after NNK). (*D*) Analysis of *Lcn2* mRNA expression by RNA-seq in normal lung tissues (blue, $n = 9$–10 per time point) with matched lesions (hyperplasias, adenomas, LUADs [red], $n = 4$–23 per time point) of *Gprc5a*$^{-/-}$ mice at end of NNK and 3 and 7 months after NNK treatment. (*E*) Analysis of LCN2 protein in BAL fluid of *Gprc5a*$^{-/-}$ mice at the different time points after NNK exposure ($n = 7$–10 per time point) by ELISA. *P* values denoting comparisons between two groups were obtained using unpaired Student's *t* test, and values for analysis of *Lcn2* expression progressively with time were obtained using ANOVA. (*F*) Representative histopathologic (H&E) and LCN2 immunoreactivity from NNK-exposed *Gprc5a*$^{-/-}$ mice with hyperplasia (left), adenoma (middle), and lung adenocarcinoma (right). Scale bars: top row, 100 μm; middle and bottom rows, 50 μm. $^{*}P < 0.05$, $^{**}P < 0.01$, and $^{***}P < 0.001$. H&E = hematoxylin and eosin; NNK = nicotine-specific nitrosamine ketone.

Elevated LCN2 in Human LUAD

We were prompted to evaluate the expression of LCN2 in human LUADs. *LCN2* was significantly elevated in human LUADs but not in lung squamous cell carcinomas (LUSCs) from the The Cancer Genome Atlas (TCGA) cohort (20, 21) compared with normal lung tissues ($P < 0.001$; Figure 2A). *LCN2* mRNA was significantly elevated in the LUADs when compared with LUSCs, and this observation was validated in the independent cohort developed by MD Anderson, PROSPECT (Profiling of Resistance Patterns and Oncogenic Signaling Pathways in Evaluation of Cancers of the Thorax [22]; $P < 0.001$; Figures 2B and 2C). *LCN2* mRNA was also significantly increased in *KRAS*-mutant LUADs (KM-LUADs) relative to *KRAS*-WT LUADs in three independent data sets (all $P < 0.05$; Figure 2D; 23–25). By immunohistochemistry analysis of a tissue microarray of 271 early-stage (stages 1–3) non–small cell lung cancer and without preoperative treatment (Figure 2E), we found that LCN2 protein was significantly upregulated in LUADs relative to LUSCs ($P < 0.001$; Figure 2F). We also found that LCN2 protein was increased in KM-LUADs that were WT for *STK11* and *TP53* when compared with LUADs that were WT for all three genes as well as for *EGFR* in our tissue microarray and in the The Cancer Genome Atlas cohort (all $P < 0.05$; Figure 2G). Despite no significant correlation between LCN2 and LUAD histologic patterns (Figures E1A and E1B), LCN2 significantly and inversely correlated with NKX2-1 in both LUAD and KM-LUAD, suggesting an association between LCN2 induction and gastric differentiation (Figures E1C and E1D), in line with previous reports (22, 26). These findings suggest that LCN2 is augmented in the pathogenesis of human LUAD.

Upregulated LCN2 Is Associated with COPD

Earlier work has shown that LCN2 is induced upon inflammation (27). *Lcn2* expression was significantly and markedly positively correlated with levels of the proinflammatory cytokines *Il1b*, *Il18*, and *Il6* (all $P < 0.05$; Figure E2A) and with an inflammation gene signature ($P < 0.001$; Figure E2B) in normal lung tissues from *Gprc5a*$^{-/-}$ mice. We were thus enticed to

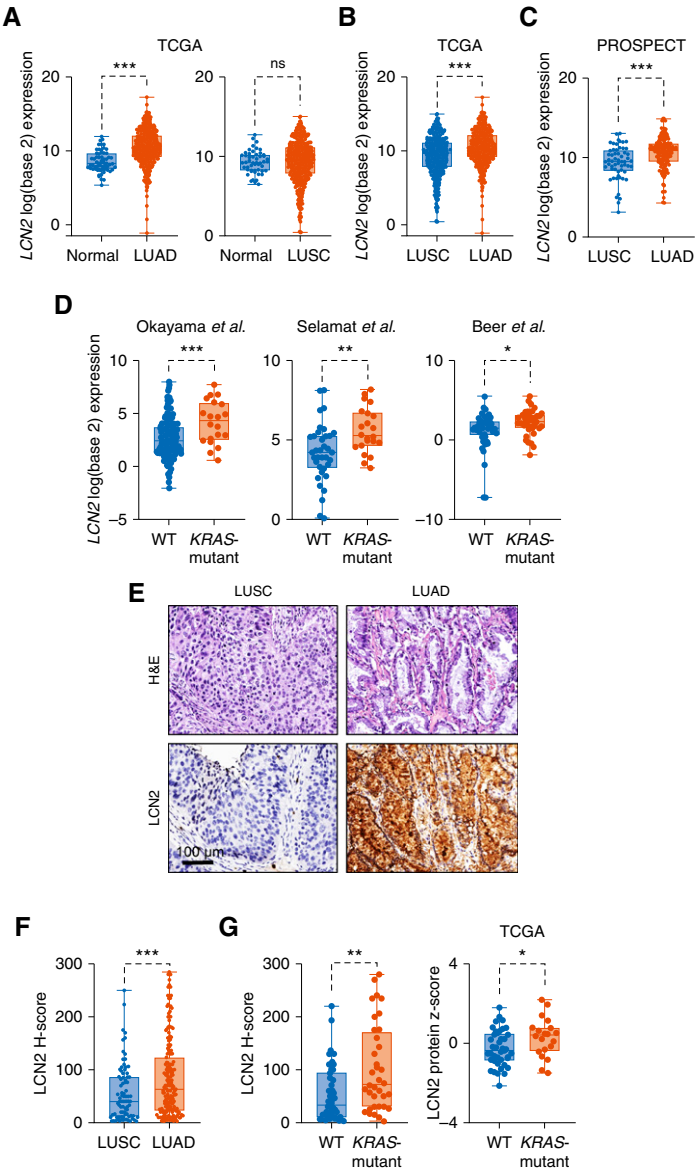

Figure 2. Elevated *LCN2* expression in human lung adenocarcinoma (LUAD). (*A*) *LCN2* mRNA levels were examined between normal lung tissues (blue, $n = 59$) and LUADs (red, $n = 514$) as well as between normal lung tissues (blue, $n = 51$) and lung squamous cancers (LUSCs) (red, $n = 502$) in the The Cancer Genoma Atlas (TCGA) data sets (20, 21). (*B*) *LCN2* mRNA levels were also directly examined between LUSCs (blue, $n = 502$) and LUADs (red, $n = 514$) in the TCGA data sets. (*C*) *LCN2* mRNA levels were statistically compared between LUSCs (blue, $n = 57$) and LUADs (red, $n = 152$) in the MD Anderson dataset, PROSPECT (Profiling of Resistance Patterns and Oncogenic Signaling Pathways in Evaluation of Cancers of the Thorax) (22). (*D*) *LCN2* mRNA levels were also statistically compared between LUADs that are wild type (WT) for *KRAS* and *KRAS*-mutant LUADs (KM-LUADs) in the following cohorts: Okayama and colleagues (blue, WT, $n = 206$; red, KM, $n = 20$); Selamat and colleagues (blue, WT, $n = 36$; red, KM, $n = 22$); Beer and colleagues (blue, WT, $n = 46$; red, KM, $n = 39$) (23–25). (*E*) Representative photomicrographs of histopathologic (H&E) and LCN2 immunohistochemical analyses of LUSC (left) and LUAD (right) specimens from the assessed tissue microarray (*see* Methods). (*F*) LCN2 protein expression was statistically compared between LUSCs (blue, $n = 84$) and LUADs (red, $n = 187$) using tumor with positive LCN2 H-scores. (*G*) LCN2 protein levels were also statistically compared between WT- and KM-LUADs in a tissue microarray using tumors with positive LCN2 H-scores (blue, WT, $n = 36$; red, KM, $n = 50$) and in TCGA reverse-phase protein array data set (blue, WT, $n = 41$; red, KM, $n = 20$). Solid horizontal lines represent median *LCN2* $\log_2$ expression values, H-scores, or protein *z*-scores. Differences in LCN2 levels between two groups were statistically assessed using the unpaired Student's *t* test. Scale bar, 100 μm. $^*P < 0.05$, $^{**}P < 0.01$, and $^{***}P < 0.001$. H&E = hematoxylin and eosin; ns = not significant.

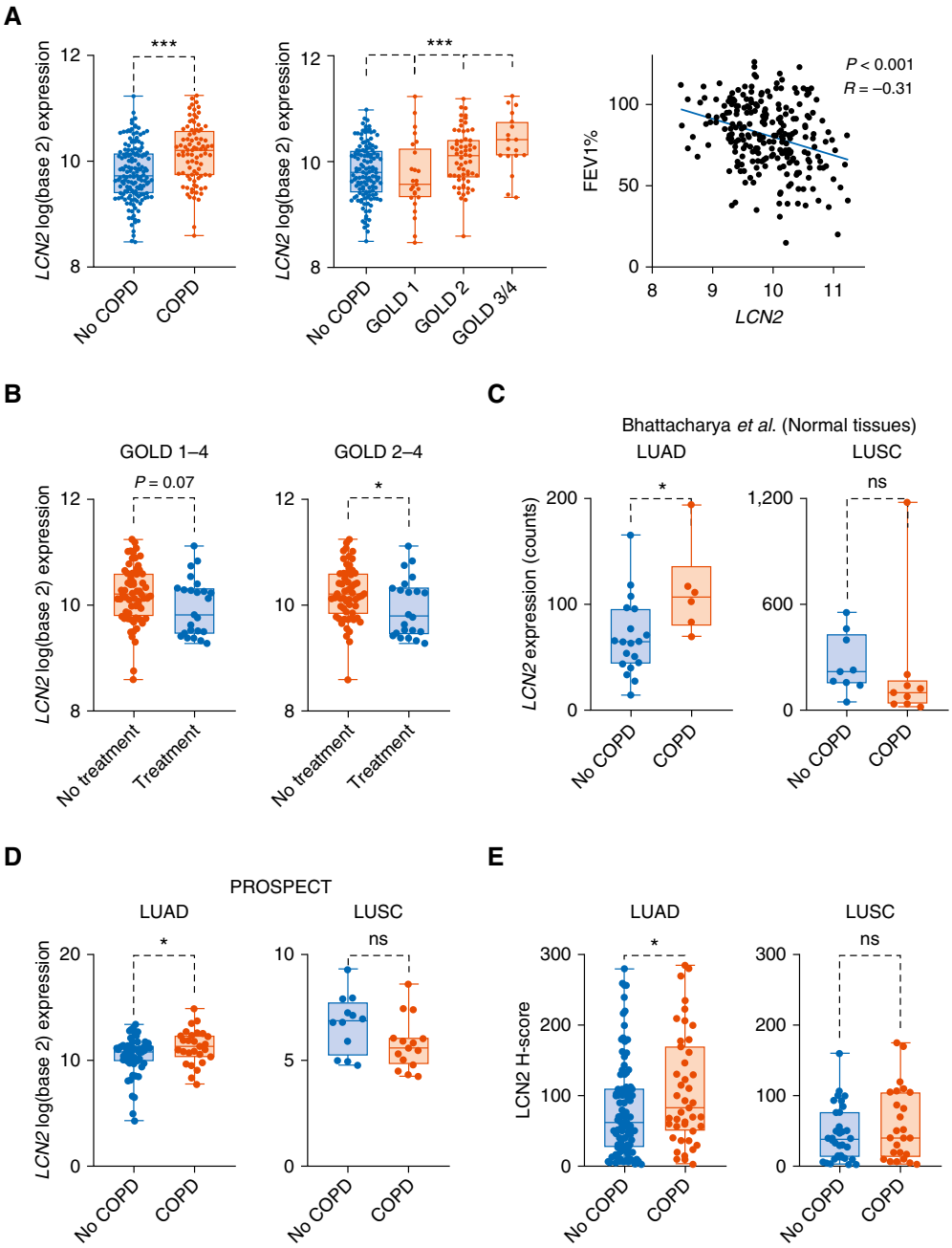

Figure 3. Upregulation of *LCN2* in human chronic obstructive pulmonary disease (COPD) and COPD-associated lung adenocarcinoma (LUAD). (*A*) *LCN2* mRNA was statistically analyzed using unpaired Student's *t* test in normal-appearing airway brushings ($n = 238$) from lung cancer–free patients in the data set by Steiling and colleagues based on COPD status (without COPD, blue, $n = 151$; with COPD, red, $n = 87$; 28). *LCN2* mRNA levels in airway brushings were also statistically assessed based on the Global Initiative for Chronic Obstructive Lung Disease (GOLD) criteria for COPD staging (middle panel; blue, no COPD, $n = 133$; red, GOLD 1–4, $n = 19$–61 per stage) using unpaired Student's *t* test. *LCN2* mRNA levels were also correlated with FEV_1 percentage using Pearson's correlation coefficient (right panel). (*B*) *LCN2* mRNA levels were statistically compared between patients without and with antiinflammatory treatment using all patients with COPD (GOLD 1–4; left panel; red, no treatment, $n = 64$; blue, treatment, $n = 23$) and patients with moderate to severe COPD (GOLD 2–4; right panel; red, no treatment, $n = 58$; blue, treatment, $n = 22$) (28) using the Student's *t* test. (*C*) *LCN2* expression was statistically compared using unpaired Student's *t* test between normal lung tissues adjacent to LUADs without (blue, $n = 19$) and with (red, $n = 6$) COPD as well as between normal lungs adjacent to lung squamous cancers (LUSCs) without (blue, $n = 9$) and with (red, $n = 9$) COPD in the data set by Bhattacharya and colleagues (29). (*D*) *LCN2* expression was statistically compared using the unpaired Student's *t* test between LUADs without (blue, $n = 58$) and with (red, $n = 27$) COPD as well as between LUSCs without (blue, $n = 12$) and with (red, $n = 15$) COPD in the MD Anderson cohort, PROSPECT (Profiling of Resistance Patterns and Oncogenic Signaling Pathways in Evaluation of Cancers of the Thorax) (22). (*E*) LCN2 H-scores were statistically compared using the unpaired Student's *t* test between LUADs from the MD Anderson tissue microarray cohort without (blue, $n = 98$) and with (red, $n = 43$) COPD and between LUSCs from the same tissue microarray without (blue, $n = 34$) and with (red, $n = 25$) COPD. $^{*}P < 0.05$ and $^{***}P < 0.001$. ns = not significant.

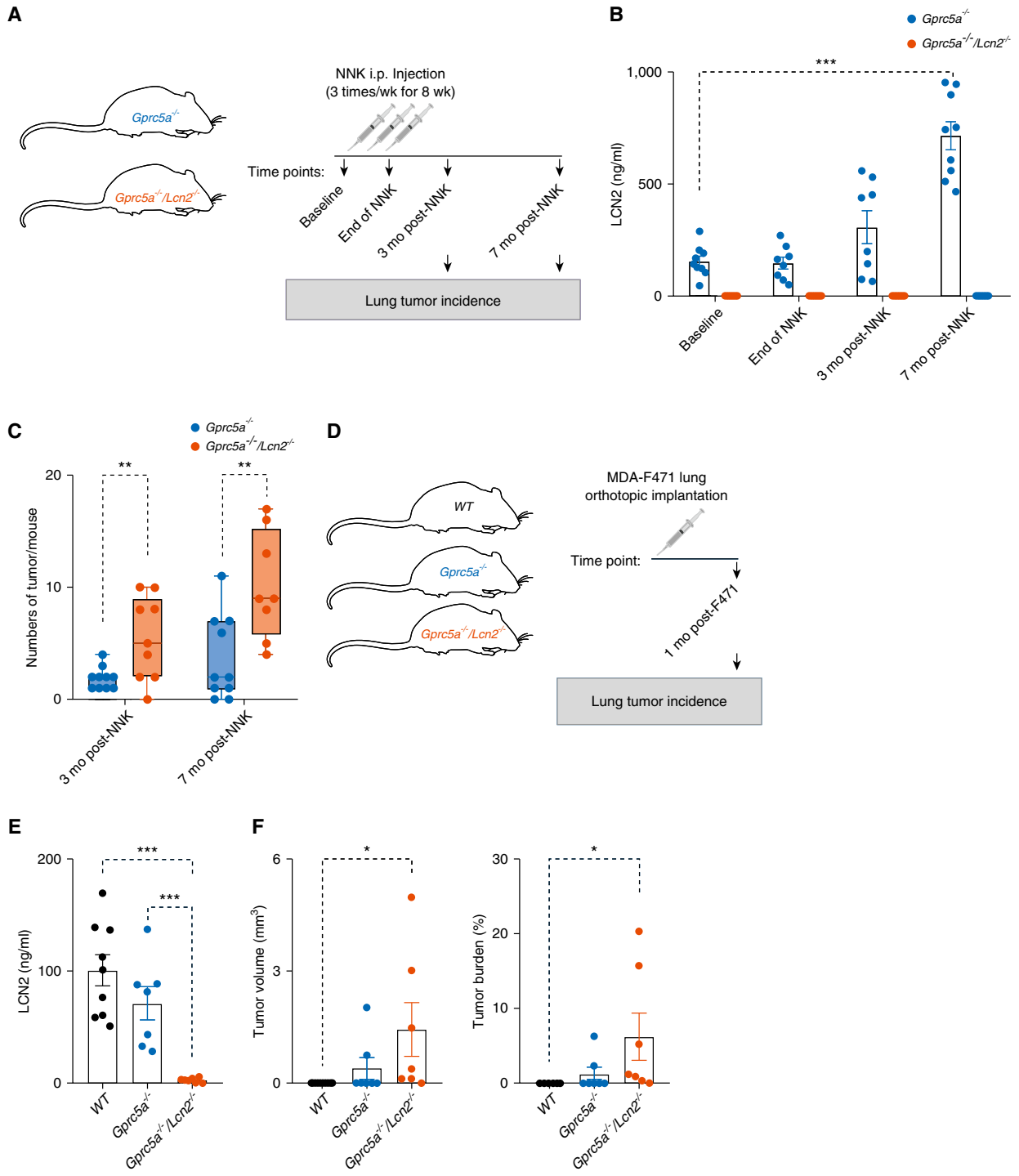

Figure 4. Loss of *Lcn2* augments lung adenocarcinoma (LUAD) development in tobacco carcinogen–exposed *Gprc5a*$^{-/-}$ mice. (*A*) Schematic timeline depicting NNK i.p. injection of 8-week-old *Gprc5a*$^{-/-}$ and *Gprc5a*$^{-/-}$/*Lcn2*$^{-/-}$ mice divided into groups of 8–10 mice (per genotype and time point) and studied at baseline, end of NNK, and 3 and 7 months after NNK treatment. (*B*) LCN2 was quantified by ELISA in BAL fluid collected from *Gprc5a*$^{-/-}$ and *Gprc5a*$^{-/-}$/*Lcn2*$^{-/-}$ mice at the indicated time points ($n = 7$–9 mice per group). (*C*) LUAD incidence (number of tumors per mouse) was statistically compared using the unpaired Student's *t* test between *Gprc5a*$^{-/-}$ and *Gprc5a*$^{-/-}$/*Lcn2*$^{-/-}$ mice ($n = 8$–10 mice per group) at 3 and 7 months after NNK. (*D*) Schematic illustrating lung orthotopic transplantation of *Gprc5a*$^{-/-}$ LUAD MDA-F471 cells (2.5×10^6 cells) in 8-week-old wild-type (WT), *Gprc5a*$^{-/-}$, and *Gprc5a*$^{-/-}$/*Lcn2*$^{-/-}$ mice ($n = 7$–9 mice per genotype) and analysis at 1 month after implantation. (*E*) LCN2 ELISA of BAL fluid obtained from the same WT, *Gprc5a*$^{-/-}$, and *Gprc5a*$^{-/-}$/*Lcn2*$^{-/-}$ mice ($n = 7$–9 mice per group) at 1 month after MDA-F471 cell implantation. (*F*) Analysis of tumor volume and tumor burden in orthotopically transplanted lungs of WT, *Gprc5a*$^{-/-}$, and *Gprc5a*$^{-/-}$/*Lcn2*$^{-/-}$ recipient mice ($n = 7$–9 mice per group). Differences between two groups were statistically examined using the unpaired Student's *t* test. $^*P < 0.05$, $^{**}P < 0.01$, and $^{***}P < 0.001$. i.p. = intraperitoneal; NNK = nicotine-specific nitrosamine ketone.

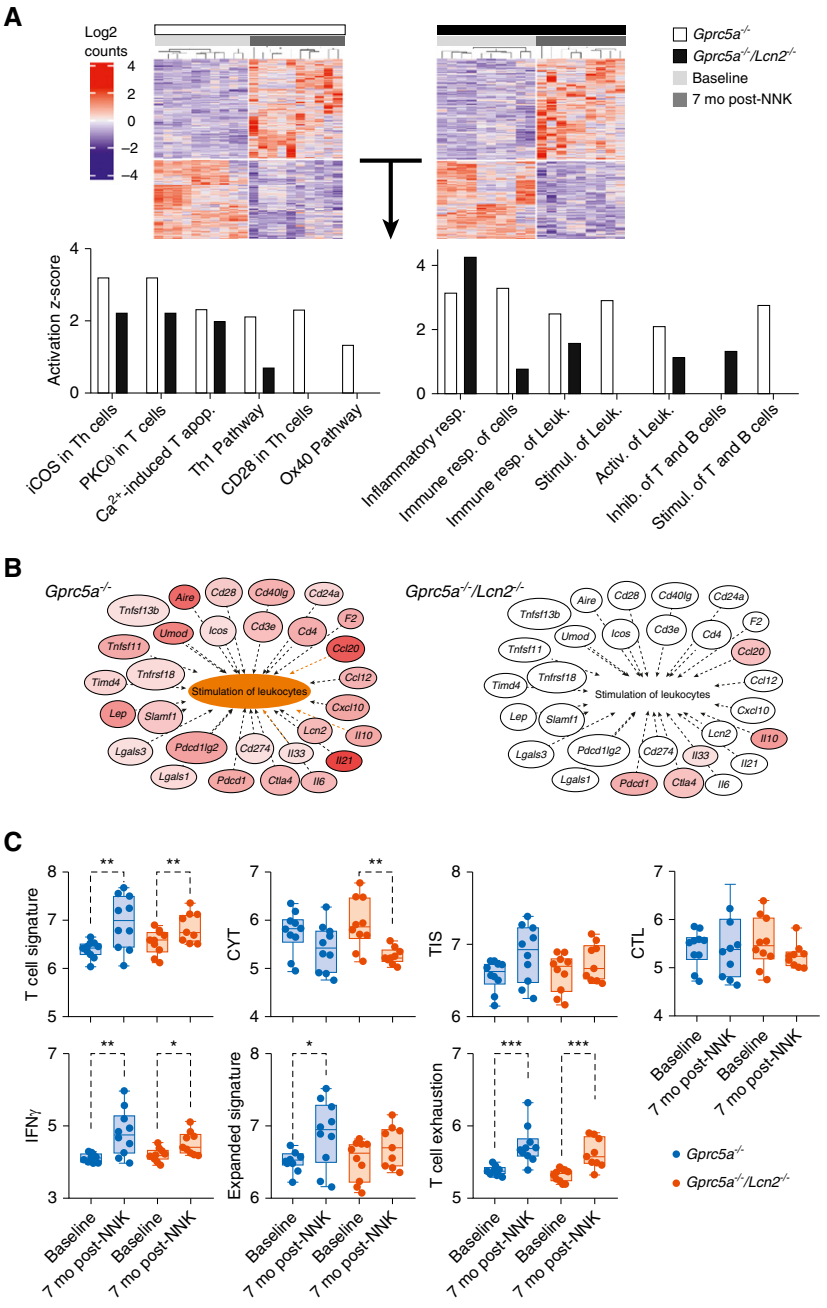

Figure 5. Loss of *Lcn2* in tobacco carcinogen–exposed *Gprc5a*$^{-/-}$ mice promotes gene expression programs associated with reduced antitumor immunity. (*A*) Differentially expressed genes between *Gprc5a*$^{-/-}$ lungs at 7 months after nicotine-specific nitrosamine ketone (NNK) compared with baseline (top left, $n = 1{,}116$ gene features) and between *Gprc5a*$^{-/-}$/*Lcn2*$^{-/-}$ lungs at the same time points (top right, $n = 775$ gene features; $n = 9$–10 mice per group) were identified by RNA-sequencing analysis as described in the online supplement section. Columns denote lung samples and rows represent gene features (red, upregulated; blue, downregulated). Pathways (bottom left) and gene sets (bottom right) enriched among *Gprc5a*$^{-/-}$ and *Gprc5a*$^{-/-}$/*Lcn2*$^{-/-}$ lung tissues with time were identified using Ingenuity Pathways Analysis (IPA) and then cross-compared and plotted. Activation of the pathway or gene set between 7 months after NNK and baseline for *Gprc5a*$^{-/-}$ (white bars) and *Gprc5a*$^{-/-}$/*Lcn2*$^{-/-}$ (black bars) is indicated by the *z*-scores. (*B*) Topological gene–gene network analysis of genes associated with stimulation of leukocytes in *Gprc5a*$^{-/-}$ (left) and *Gprc5a*$^{-/-}$/*Lcn2*$^{-/-}$ (right) lungs at 7 months after NNK compared with baseline (red, upregulated) were derived using IPA. Predicted activation of leukocyte stimulation based on the gene set is indicated by the orange color (in *Gprc5a*$^{-/-}$ mice). (*C*) The following T-cell signatures indicative of

interrogate lung *LCN2* in the context of COPD, a pulmonary disorder typified by inflammation (4). By analysis of a public data set of normal-appearing airway brushings from smokers with and without COPD (28), we found that *LCN2* was significantly higher in patients with COPD relative to smokers without the disease ($P < 0.001$; Figure 3A, left). *LCN2* was also significantly progressively increased with COPD stage ($P < 0.001$; Figure 3A, middle) and inversely correlated with FEV_1% ($P < 0.001$, $R = -0.31$; Figure 3A, right). Patients with COPD who received antiinflammatory treatment by inhalation exhibited reduced airway expression of *LCN2*, an association that reached statistical significance when tested in patients with moderate to severe COPD ($P < 0.05$; Figure 3B, right). In an independent data set (29), we found that *LCN2* was significantly elevated in normal tissues adjacent to COPD-associated LUADs compared with uninvolved tissues from patients with LUAD without COPD ($P < 0.05$; Figure 3C). In an independent cohort (PROSPECT [22]), *LCN2* was also significantly elevated in patients with COPD-associated LUADs compared with those without COPD ($P < 0.05$; Figure 3D). Furthermore, immunohistochemical analysis demonstrated significantly higher LCN2 protein in patients with LUADs with COPD compared with those without COPD ($P < 0.05$; Figure 3E). None of these effects were observed when LCN2 was assessed in uninvolved normal tissues or tumors from patients with LUSC (Figures 3C–3E). There were no significant differences in LUAD histological patterns between patients with and without COPD (Figure E3). Of note, even among KM-LUADs, LCN2 protein was significantly increased in COPD-associated LUADs relative to tumors without COPD ($P < 0.05$, Figure E4). These findings suggest that elevated LCN2 is a molecular feature of COPD and COPD-associated LUAD.

Increased Lung Tumor Development in *Gprc5a*$^{-/-}$ Mice with Knockout of *Lcn2*

We generated *Gprc5a*$^{-/-}$ mice with knockout of *Lcn2* (*Gprc5a*$^{-/-}$/*Lcn2*$^{-/-}$) and then compared NNK-associated temporal lung tumor development between age- and sex-matched *Gprc5a*$^{-/-}$ and *Gprc5a*$^{-/-}$/*Lcn2*$^{-/-}$ littermates (8–10 mice per group) (Figure 4A). We confirmed

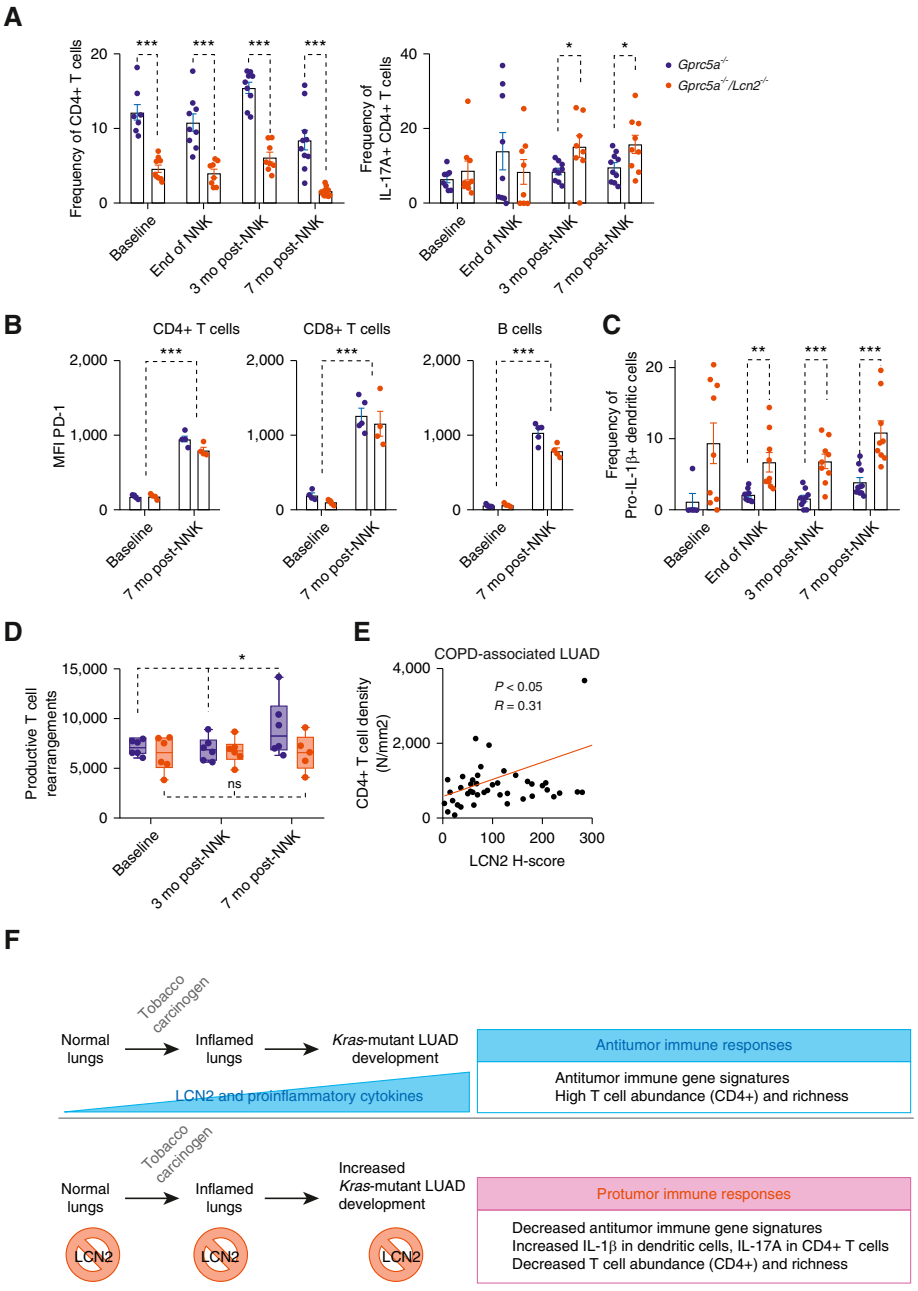

Figure 6. Loss of *Lcn2* decreases T-cell abundance and elevates proinflammatory cytokines during lung adenocarcinoma (LUAD) development. (*A*) Flow cytometry analysis of total (left) and IL-17A–expressing CD4$^+$ T cells (right) in lungs of *Gprc5a*$^{-/-}$ (blue) and *Gprc5a*$^{-/-}$/*Lcn2*$^{-/-}$ (red)

significant and progressive upregulation of LCN2 in BAL fluid of *Gprc5a*$^{-/-}$ mice, which was absent in the *Gprc5a*$^{-/-}$/*Lcn2*$^{-/-}$ littermates ($P < 0.001$; Figure 4B). Intriguingly, we found that *Gprc5a*$^{-/-}$/*Lcn2*$^{-/-}$ mice exhibited significantly increased lung tumor development at both 3 and 7 months after NNK (both $P < 0.01$; Figures 4C and E5A). Relative to WT ($n = 9$) and *Gprc5a*$^{-/-}$ ($n = 7$) mice, *Gprc5a*$^{-/-}$/*Lcn2*$^{-/-}$ littermates ($n = 7$) transplanted with *Gprc5a*$^{-/-}$ LUAD cells (MDA-F471) (30) exhibited elevated lung tumor volumes and burden (Figures 4D–4F). Also, compared with control shRNA-transduced cells, MDA-F471 cells with stable knockdown of *Lcn2* exhibited increased activating phosphorylation of AKT and ERK1/2 both basally and in response to treatment with 50 ng/ml epidermal growth factor (Figures E5B and E5C). Our findings demonstrate that inhibition of early induction of *Lcn2* markedly augments LUAD development.

Loss of *Lcn2* Suppresses Gene Expression Programs Associated with Antitumor Immunity

We next sought to pinpoint gene expression alterations associated with *Lcn2* during LUAD pathogenesis. We performed RNA-seq analysis of baseline normal lung and tumor-bearing tissues at 7 months after NNK in *Gprc5a*$^{-/-}$ and *Gprc5a*$^{-/-}$/*Lcn2*$^{-/-}$ littermates ($n = 9$–10 mice per group). We identified 1,116 (Table E2) and 775 (Table E3) differentially expressed genes (adjusted *P* value <0.05) in *Gprc5a*$^{-/-}$ and *Gprc5a*$^{-/-}$/*Lcn2*$^{-/-}$ littermates, respectively (Figure 5A, top). Relative to *Gprc5a*$^{-/-}$ littermates, *Gprc5a*$^{-/-}$/*Lcn2*$^{-/-}$ tumor-bearing lungs exhibited overall reduced activation of antitumor immune phenotypes (Figure 5A, bottom left) and gene sets (Figure 5A, bottom right). Genes indicative of immune cell infiltration or reactivity (e.g., *Cd3e*, *Cd4*, *Cd40lg*) were increased in *Gprc5a*$^{-/-}$ tumor-bearing lungs, contrary to their distinct lack of modulation in *Gprc5a*$^{-/-}$/*Lcn2*$^{-/-}$ littermates (Figure 5B). Tumor-bearing lungs from both groups exhibited similar levels of multiple immune checkpoints including *Ctla4* and *Pdcd1* (Figure 5B). Analysis of signatures indicative of T-cell states (*see* online supplement) showed that relative to baseline, tumor-bearing lungs from only *Gprc5a*$^{-/-}$ mice displayed significantly activated T-cell and expanded T-cell

Figure 5. (*Continued*). different phenotypes were propagated and computed for each sample as described in the online supplement: CTL = cytotoxic T lymphocyte; CYT = T cell, cytolytic activity; TIS = tumor inflammation signature; IFN-γ; and T-cell expanded and T-cell exhaustion signatures. The T-cell signatures were then statistically compared between *Gprc5a*$^{-/-}$ and *Gprc5a*$^{-/-}$/*Lcn2*$^{-/-}$ lungs at baseline and at 7 months after NNK. *P* values were calculated between *Gprc5a*$^{-/-}$ lung tissues (blue) at baseline and 7 months after NNK as well as between *Gprc5a*$^{-/-}$/*Lcn2*$^{-/-}$ lungs (red) at the same time points using the unpaired Student's *t* test. *$P < 0.05$, **$P < 0.01$, and ***$P < 0.001$. Activ. = activation; apop. = apoptosis; iCOS = inducible T-cell costimulator; Inhib. = inhibition; Leuk. = leukocytes; PKC = protein kinase C; resp. = response; Stimul. = stimulation; Th1 = T-helper cell type 1.

signatures, which is in contrast to suppressed cytotoxic T-cell activity in *Gprc5a*$^{-/-}$/*Lcn2*$^{-/-}$ lungs (Figure 5C). IFN-γ and T-cell exhaustion signatures were increased in tumor-bearing lungs irrespective of *Lcn2* genetic background. Additionally, deconvolution of immune infiltration (*see* Supplementary Methods) revealed significantly reduced neutrophil ($P < 0.001$) and CD4$^+$ T-cell ($P < 0.05$) abundance in *Gprc5a*$^{-/-}$/*Lcn2*$^{-/-}$ relative to *Gprc5a*$^{-/-}$ lungs at baseline (Figure E6). These data suggest attenuated antitumor immune responses during LUAD development upon loss of *Lcn2*.

Loss of *Lcn2* Modulates Host Immune Responses during Lung Oncogenesis

We next interrogated temporal immune responses during LUAD development in *Gprc5a*$^{-/-}$ and *Gprc5a*$^{-/-}$/*Lcn2*$^{-/-}$ mice. Although both groups exhibited gradual increases with time in CD8$^+$ T-cell abundance (Figure E7A), *Gprc5a*$^{-/-}$/*Lcn2*$^{-/-}$ relative to *Gprc5a*$^{-/-}$ lungs exhibited significantly suppressed abundance of CD4$^+$ T cells across all time points (all $P < 0.001$; Figure 6A, left). Tumor-bearing lungs of *Gprc5a*$^{-/-}$/*Lcn2*$^{-/-}$ relative to *Gprc5a*$^{-/-}$ littermates mice exhibited significantly higher levels of IL-17A–expressing CD4$^+$ T cells at 3 and 7 months after NNK (both $P < 0.05$; Figure 6A, right). PD-1 expression on T/B cells was significantly increased (all $P < 0.001$) in tumor-bearing lungs compared with baseline in both *Gprc5a*$^{-/-}$ and *Gprc5a*$^{-/-}$/*Lcn2*$^{-/-}$ mice (Figure 6B), consistent with our RNA-seq analysis (Figures 5B and 5C). Relative to *Gprc5a*$^{-/-}$ littermates, lung dendritic cells in *Gprc5a*$^{-/-}$/*Lcn2*$^{-/-}$ mice exhibited significantly elevated expression of IL-1β (all $P < 0.01$; Figure 6C) and PD-1/PD-L1 (all $P < 0.05$; Figure E7B). Also, normal (nonmalignant) lung tissue from *Gprc5a*$^{-/-}$/*Lcn2*$^{-/-}$ mice exhibited more pronounced inflammatory lesions (Figure E7C). Additionally, sequencing analysis revealed significantly enhanced productive T-cell receptor rearrangements in *Gprc5a*$^{-/-}$ but not *Gprc5a*$^{-/-}$/*Lcn2*$^{-/-}$ tumor-bearing lungs at 7 months after NNK ($P < 0.05$; Figure 6D). Furthermore, LCN2 protein positively and significantly correlated with CD4$^+$ T-cell density among early-stage preoperatively untreated COPD-associated LUADs ($P < 0.05$, $R = 0.31$; Figure 6E). In an independent data set of COPD-associated LUAD, *LCN2* was significantly positively correlated with host defense markers (*CXCL1*, *DEFB1*, *SAA1*, and *FCGR3B*) and the IL-1 decoy receptor *IL1R2*, as well as significantly inversely correlated with protumor immune markers (*CCL2*, *CCL22*, *IL6ST*) and oncogenic antigens (*CEACAM5*, *CEACAM6*) (all $P < 0.05$; Figures E8A and E8B). Our data demonstrate that inhibition of *Lcn2* induction elevates protumor inflammatory signaling while augmenting lung tumor development.

Discussion

Here we found that *Lcn2* was elevated in normal and malignant lung tissues during LUAD development and highly correlated with proinflammatory cytokines and signatures. *LCN2* was also significantly increased in human LUADs but not in LUSCs compared with normal tissues and was a molecular feature of KM-LUAD and COPD. We further found that loss of *Lcn2* in lung tumor–prone mice exacerbated LUAD development with evidence of compromised antitumor immunity and heightened protumor inflammatory phenotypes. Our findings point to a novel protective role for *Lcn2* in which we hypothesize that augmented lung LCN2 counteracts LUAD development (Figure 6F).

Our findings are in line with reports showing augmented LCN2 and its possible protective roles during inflammatory states (27), including in the lung (31, 32). Previous studies underscored the important role of LCN2 in airway defense, particularly in attenuating inflammation and in pathogen clearance (31, 32). It is thus plausible to surmise that upregulated expression of LCN2 during early phases of lung oncogenesis is likely a host defense mechanism (against genetic insults, tobacco smoke, and/or inflammation) that helps to limit protumor inflammatory cues (Figure 6F). This supposition is in line with previous work showing that *Lcn2* loss in *Il10*$^{-/-}$ mice enhanced the progression of colitis to colon cancer and elevated the expression of the proinflammatory cytokine IL-6 (27). Of note, we found that *LCN2* was elevated in normal lung tissues and LUADs from patients with COPD, a disease typified by pulmonary inflammation and that increases the risk for developing lung malignancy (33). These findings are in close agreement with a previous study showing elevated LCN2 in plasma of patients with COPD compared with healthy subjects (34). Thus, it is conceivable that *LCN2* is a biomarker of COPD—with higher expression indicating elevated inflammation and, perhaps, increased likelihood of progression to lung cancer. Interestingly, we found that LCN2 expression in human COPD-associated LUAD positively correlated with markers of host defense (e.g., *DEFB1*) and was inversely correlated with levels of oncogenic antigens (e.g., *CEACAM5*) and gene features of protumor immunity (e.g., *CCL2*). Given our findings, it is conceivable that *LCN2* may prevent the

Figure 6. (*Continued*). mice at baseline, end of NNK exposure, and at 3 and 7 months after NNK ($n = 8$–10 mice per group). (*B*) Flow cytometry analysis of PD-1 in CD4$^+$ (left) and CD8$^+$ (middle) T cells as well as in B cells (right) from lungs of *Gprc5a*$^{-/-}$ (blue) and *Gprc5a*$^{-/-}$/*Lcn2*$^{-/-}$ (red) mice at baseline and at 7 months after NNK ($n = 4$–5 per group). (*C*) Flow cytometry analysis of pro-IL-1β in dendritic cells from *Gprc5a*$^{-/-}$ (blue) and *Gprc5a*$^{-/-}$/*Lcn2*$^{-/-}$ (red) lungs before and after NNK exposure ($n = 8$–10 mice per group). Differences were statistically assessed between the two genotypes within time points using unpaired Student's *t* test. (*D*) T-cell receptor β (TCRβ) sequencing was performed as described in the online supplement. Time-dependent changes in productive TCR rearrangements were statistically evaluated for *Gprc5a*$^{-/-}$ (blue) and *Gprc5a*$^{-/-}$/*Lcn2*$^{-/-}$ (red) lungs ($n = 5$–6 mice per group) using ANOVA. $^*P < 0.05$, $^{**}P < 0.01$, and $^{***}P < 0.001$. (*E*) Correlation between CD4$^+$ T-cell density and LCN2 H-scores in LUADs with chronic obstructive pulmonary disease (COPD) ($n = 43$) was statistically interrogated using Pearson's correlation coefficient. (*F*) Schematic summarizing the study's main findings. *Lcn2* expression in both normal-appearing lung tissues and tumors was augmented during tobacco carcinogen–associated LUAD development in *Gprc5a*$^{-/-}$ mice and correlated with markers of inflammation. Human LCN2 was upregulated in LUAD but not in lung squamous cancer when compared with normal lung, and its expression in normal tissues or tumors was associated with COPD. Genetic deletion of *Lcn2* in *Gprc5a*$^{-/-}$ mice increased tobacco carcinogen–associated lung tumor development and protumor immune phenotypes exemplified by decreased antitumor immune gene signatures, increased proinflammatory cytokine production by CD4$^+$ T cells and myeloid cells, and reduced T-cell richness—overall suggestive of a protective role for *LCN2* induction in LUAD pathogenesis. MFI = mean fluorescence intensity; NNK = nicotine-specific nitrosamine ketone.

progression of COPD to lung cancer, a conjecture that warrants future studies.

A notable observation in our study was the specific elevated expression of LCN2 in LUAD but not in LUSC even among patients with COPD. LUADs and LUSCs are thought to arise from distinct anatomical regions and cells of origin (1). Whereas LUSCs tend to develop more proximally in the lung (upper airways), LUADs commonly arise from the lung periphery (1). Also, LUSCs are thought to develop from basal (including bronchiolar) cells, whereas alveolar and airway secretory (e.g., club) cells are alleged cells of origin for LUADs (35, 36). Increased *LCN2* expression has been reported in airway goblet cells and alveolar type II pneumocytes of inflamed lungs (37). Also, single-cell analysis of murine lungs work revealed that *Lcn2* was abundantly expressed in alveolar type II cells (38). We found that LCN2 was inversely correlated with the lineage-specific oncogene NKX2-1 in LUAD, suggesting that LCN2 may be associated with LUADs that exhibit increased gastric differentiation (22). It is plausible that airway lineage-specific cues may account for the distinctive upregulation of *LCN2* in LUAD and for the inflammation-associated host defense roles of this lipocalin in LUAD evolution.

LCN2 has been classically described as an immunomodulator in neutrophils (39). LCN2 was also shown to be induced in other myeloid cells, such as dendritic cells (40), upon lung inflammation and infection (41). Thus, although we showed that *LCN2* is highly expressed in lung tissues, distinct roles for this lipocalin in nonepithelial subsets and particularly immune cells cannot be discounted, especially because our murine models comprised nonconditional knockout of host *Lcn2*. Also, our bulk RNA-seq analysis of mouse lung tissues did not discriminate signaling cues in epithelial and neutrophil compartments. Nonetheless, we present multiple lines of evidence that LCN2 plays major roles in the lung epithelium during LUAD pathogenesis. LCN2 was highly expressed in murine and human airway and tumor cells, including those from patients with COPD and LUAD, and *in vitro* knockdown of its expression increased LUAD cell proliferation and survival signaling. Our findings are in line with earlier work showing that LCN2 is highly expressed in lung epithelial cells in response to inflammation (37). Future studies are warranted to delineate epithelial- versus neutrophil-derived host defense roles of LCN2 in LUAD development.

LCN2 was reported to be central in maintaining a T-helper cell type 1 (Th1) phenotype (40). Also, loss of *Lcn2* was shown to attenuate proliferation of T cells in models of autoimmune encephalomyelitis (42). It is important to accentuate that our study demonstrated that loss of *Lcn2* augmented proinflammatory cytokine (IL-1β and IL-17A) expression by immune cells. Indeed, IL-17A has been attributed critical roles in mediating COPD-type chronic inflammation after prolonged smoke exposure and in promoting lung tumorigenesis in inflammation-associated LUAD models (43, 44). We found that *Gprc5a*$^{-/-}$ mice with *Lcn2* deletion exhibited increased IL-1β expression in myeloid cells. We also previously demonstrated that targeting proinflammatory cytokines reduced LUAD development concomitant with elevated Th1 and cytolytic immune responses (7, 45). Interestingly, earlier work showed that LCN2 attenuated nuclear factor-κB (NF-κB)-mediated signaling and proinflammatory cytokine production in macrophages and retinal tissue (46, 47). It is reasonable to surmise that induction of LCN2 during early phases of lung oncogenesis restricts proinflammatory signatures, which in turn leads to sustenance of antitumor immune phenotypes. Future studies are warranted to further explore the immunomodulatory role of LCN2 in LUAD development.

Previous studies underscored tumor promoting roles for LCN2 (48). For instance, disruption of *Lcn2* was shown to suppress metastasis of murine breast cancer (15). Whereas these reports mostly focused on advanced cancers and mechanisms of tumor progression and metastasis, our study centered on early pathogenesis of LUAD. Our findings are in accordance with the report by Moschen and colleagues in which *Lcn2* deletion resulted in early development of colorectal tumors in mice with inflammatory colitis (27). Of note, LCN2 was previously shown to be elevated in lung tumors (49, 50)—an observation that we describe herein and that, at first glance, may provoke a supposition that the lipocalin is a lung oncogene. Based on our findings, we suggest that increased LCN2 in patients with overt lung lesions is in response to proinflammatory cues. It is plausible that similar proinflammatory signals lead to induction of LCN2 in lung inflammatory diseases such as COPD and in early phases of LUAD development—for instance, through NF-κB and JAK/STAT pathways as described by earlier reports (46, 47). However, it cannot be neglected that human LUADs still arise despite high expression of LCN2, possibly suggesting escape mechanisms from LCN2-mediated protective roles or alternative context-dependent roles for LCN2 in later stages of LUAD progression (e.g., metastasis), which warrant further investigation.

Our study suggests that augmented LCN2 is a molecular feature of COPD and LUAD. Our findings also point to novel host defense cues in counteracting tumor-promoting immune responses and development of LUAD, thus paving the way for identification of new phenotypic targets for early detection and management of this malignancy in high-risk smokers (e.g., patients with COPD). ■

Author disclosures are available with the text of this article at www.atsjournals.org.

Acknowledgment: The authors thank Baohua Sun in Dr. Luisa Solis's laboratory for assistance with immunohistochemical staining of tissue microarrays.

References

1. Kadara H, Scheet P, Wistuba II, Spira AE. Early events in the molecular pathogenesis of lung cancer. *Cancer Prev Res (Phila)* 2016;9: 518–527.
2. Saab S, Zalzale H, Rahal Z, Khalifeh Y, Sinjab A, Kadara H. Insights into lung cancer immune-based biology, prevention, and treatment. *Front Immunol* 2020;11:159.
3. Keith RL, Miller YE. Lung cancer chemoprevention: current status and future prospects. *Nat Rev Clin Oncol* 2013;10:334–343.
4. Houghton AM. Mechanistic links between COPD and lung cancer. *Nat Rev Cancer* 2013;13:233–245.
5. O'Callaghan DS, O'Donnell D, O'Connell F, O'Byrne KJ. The role of inflammation in the pathogenesis of non-small cell lung cancer. *J Thorac Oncol* 2010;5:2024–2036.

6. Ridker PM, MacFadyen JG, Thuren T, Everett BM, Libby P, Glynn RJ; CANTOS Trial Group. Effect of interleukin-1β inhibition with canakinumab on incident lung cancer in patients with atherosclerosis: exploratory results from a randomised, double-blind, placebo-controlled trial. *Lancet* 2017;390:1833–1842.
7. Caetano MS, Zhang H, Cumpian AM, Gong L, Unver N, Ostrin EJ, *et al*. IL6 blockade reprograms the lung tumor microenvironment to limit the development and progression of K-ras-mutant lung cancer. *Cancer Res* 2016;76:3189–3199.
8. Akbay EA, Koyama S, Liu Y, Dries R, Bufe LE, Silkes M, *et al*. Interleukin-17A promotes lung tumor progression through neutrophil attraction to tumor sites and mediating resistance to PD-1 blockade. *J Thorac Oncol* 2017;12:1268–1279.
9. Iwasaki A, Foxman EF, Molony RD. Early local immune defences in the respiratory tract. *Nat Rev Immunol* 2017;17:7–20.
10. Leiva-Juárez MM, Kolls JK, Evans SE. Lung epithelial cells: therapeutically inducible effectors of antimicrobial defense. *Mucosal Immunol* 2018;11:21–34.
11. Coussens LM, Werb Z. Inflammation and cancer. *Nature* 2002;420: 860–867.
12. Tao Q, Fujimoto J, Men T, Ye X, Deng J, Lacroix L, *et al*. Identification of the retinoic acid-inducible Gprc5a as a new lung tumor suppressor gene. *J Natl Cancer Inst* 2007;99:1668–1682.
13. Fujimoto J, Nunomura-Nakamura S, Liu Y, Lang W, McDowell T, Jakubek Y, *et al*. Development of Kras mutant lung adenocarcinoma in mice with knockout of the airway lineage-specific gene Gprc5a. *Int J Cancer* 2017;141:1589–1599.
14. Hassane MTW, McDowell TL, Sivakumar S, Lang W, Ochieng JK, Nunomura-Nakamura S, *et al*. Host lipocalin 2 protects against Kras mutant lung cancer development by maintaining an anti-tumor immune contexture [abstract]. *Cancer Res* 2019;79: A4952.
15. Leng X, Ding T, Lin H, Wang Y, Hu L, Hu J, *et al*. Inhibition of lipocalin 2 impairs breast tumorigenesis and metastasis. *Cancer Res* 2009;69: 8579–8584.
16. Nikitin AY, Alcaraz A, Anver MR, Bronson RT, Cardiff RD, Dixon D, *et al*. Classification of proliferative pulmonary lesions of the mouse: recommendations of the mouse models of human cancers consortium. *Cancer Res* 2004;64:2307–2316.
17. Parra ER, Behrens C, Rodriguez-Canales J, Lin H, Mino B, Blando J, *et al*. Image analysis-based assessment of PD-L1 and tumor-associated immune cells density supports distinct intratumoral microenvironment groups in non-small cell lung carcinoma patients. *Clin Cancer Res* 2016;22:6278–6289.
18. Tang C, Hobbs B, Amer A, Li X, Behrens C, Canales JR, *et al*. Development of an immune-pathology informed radiomics model for non-small cell lung cancer. *Sci Rep* 2018;8:1922.
19. Vogelmeier CF, Criner GJ, Martinez FJ, Anzueto A, Barnes PJ, Bourbeau J, *et al*. Global strategy for the diagnosis, management, and prevention of chronic obstructive lung disease 2017 report: GOLD executive summary. *Am J Respir Crit Care Med* 2017;195:557–582.
20. Cancer Genome Atlas Research Network. Comprehensive molecular profiling of lung adenocarcinoma. *Nature* 2014;511:543–550. [Published erratum appears in *Nature* 514:262.]
21. Cancer Genome Atlas Research Network. Comprehensive genomic characterization of squamous cell lung cancers. *Nature* 2012; 489:519–525. [Published erratum appears in *Nature* 491: 288.]
22. Skoulidis F, Byers LA, Diao L, Papadimitrakopoulou VA, Tong P, Izzo J, *et al*. Co-occurring genomic alterations define major subsets of KRAS-mutant lung adenocarcinoma with distinct biology, immune profiles, and therapeutic vulnerabilities. *Cancer Discov* 2015;5: 860–877.
23. Okayama H, Kohno T, Ishii Y, Shimada Y, Shiraishi K, Iwakawa R, *et al*. Identification of genes upregulated in ALK-positive and EGFR/KRAS/ALK-negative lung adenocarcinomas. *Cancer Res* 2012;72: 100–111.
24. Selamat SA, Chung BS, Girard L, Zhang W, Zhang Y, Campan M, *et al*. Genome-scale analysis of DNA methylation in lung adenocarcinoma and integration with mRNA expression. *Genome Res* 2012;22: 1197–1211.
25. Beer DG, Kardia SL, Huang CC, Giordano TJ, Levin AM, Misek DE, *et al*. Gene-expression profiles predict survival of patients with lung adenocarcinoma. *Nat Med* 2002;8:816–824.
26. Snyder EL, Watanabe H, Magendantz M, Hoersch S, Chen TA, Wang DG, *et al*. Nkx2-1 represses a latent gastric differentiation program in lung adenocarcinoma. *Mol Cell* 2013;50:185–199.
27. Moschen AR, Gerner RR, Wang J, Klepsch V, Adolph TE, Reider SJ, *et al*. Lipocalin 2 protects from inflammation and tumorigenesis associated with gut microbiota alterations. *Cell Host Microbe* 2016; 19:455–469.
28. Steiling K, van den Berge M, Hijazi K, Florido R, Campbell J, Liu G, *et al*. A dynamic bronchial airway gene expression signature of chronic obstructive pulmonary disease and lung function impairment. *Am J Respir Crit Care Med* 2013;187:933–942.
29. Bhattacharya S, Srisuma S, Demeo DL, Shapiro SD, Bueno R, Silverman EK, *et al*. Molecular biomarkers for quantitative and discrete COPD phenotypes. *Am J Respir Cell Mol Biol* 2009;40: 359–367.
30. Fujimoto J, Kadara H, Men T, van Pelt C, Lotan D, Lotan R. Comparative functional genomics analysis of NNK tobacco-carcinogen induced lung adenocarcinoma development in Gprc5a-knockout mice. *PLoS One* 2010;5:e11847.
31. Chan YR, Liu JS, Pociask DA, Zheng M, Mietzner TA, Berger T, *et al*. Lipocalin 2 is required for pulmonary host defense against Klebsiella infection. *J Immunol* 2009;182:4947–4956.
32. Wu H, Santoni-Rugiu E, Ralfkiaer E, Porse BT, Moser C, Høiby N, *et al*. Lipocalin 2 is protective against E. coli pneumonia. *Respir Res* 2010; 11:96.
33. Mannino DM, Aguayo SM, Petty TL, Redd SC. Low lung function and incident lung cancer in the United States: data from the First National Health and Nutrition Examination Survey follow-up. *Arch Intern Med* 2003;163:1475–1480.
34. Eagan TM, Damås JK, Ueland T, Voll-Aanerud M, Mollnes TE, Hardie JA, *et al*. Neutrophil gelatinase-associated lipocalin: a biomarker in COPD. *Chest* 2010;138:888–895.
35. Spella M, Lilis I, Pepe MA, Chen Y, Armaka M, Lamort AS, *et al*. Club cells form lung adenocarcinomas and maintain the alveoli of adult mice. *Elife* 2019;8:e45571.
36. Yatabe Y. EGFR mutations and the terminal respiratory unit. *Cancer Metastasis Rev* 2010;29:23–36.
37. Cowland JB, Sørensen OE, Sehested M, Borregaard N. Neutrophil gelatinase-associated lipocalin is up-regulated in human epithelial cells by IL-1 beta, but not by TNF-alpha. *J Immunol* 2003;171: 6630–6639.
38. Treutlein B, Brownfield DG, Wu AR, Neff NF, Mantalas GL, Espinoza FH, *et al*. Reconstructing lineage hierarchies of the distal lung epithelium using single-cell RNA-seq. *Nature* 2014;509:371–375.
39. Kjeldsen L, Bainton DF, Sengeløv H, Borregaard N. Identification of neutrophil gelatinase-associated lipocalin as a novel matrix protein of specific granules in human neutrophils. *Blood* 1994;83: 799–807.
40. Floderer M, Prchal-Murphy M, Vizzardelli C. Dendritic cell-secreted lipocalin2 induces CD8+ T-cell apoptosis, contributes to T-cell priming and leads to a TH1 phenotype. *PLoS One* 2014;9: e101881.
41. Cramer EP, Dahl SL, Rozell B, Knudsen KJ, Thomsen K, Moser C, *et al*. Lipocalin-2 from both myeloid cells and the epithelium combats *Klebsiella pneumoniae* lung infection in mice. *Blood* 2017;129: 2813–2817.
42. Nam Y, Kim JH, Seo M, Kim JH, Jin M, Jeon S, *et al*. Lipocalin-2 protein deficiency ameliorates experimental autoimmune encephalomyelitis: the pathogenic role of lipocalin-2 in the central nervous system and peripheral lymphoid tissues. *J Biol Chem* 2014;289:16773–16789.
43. Chang SH, Mirabolfathinejad SG, Katta H, Cumpian AM, Gong L, Caetano MS, *et al*. T helper 17 cells play a critical pathogenic role in lung cancer. *Proc Natl Acad Sci USA* 2014;111:5664–5669.
44. Chen K, Pociask DA, McAleer JP, Chan YR, Alcorn JF, Kreindler JL, *et al*. IL-17RA is required for CCL2 expression, macrophage recruitment, and emphysema in response to cigarette smoke. *PLoS One* 2011;6:e20333.

45. Caetano MS, Hassane M, Van HT, Bugarin E, Cumpian AM, McDowell CL, *et al*. Sex specific function of epithelial STAT3 signaling in pathogenesis of K-ras mutant lung cancer. *Nat Commun* 2018;9:4589.
46. Guo H, Jin D, Chen X. Lipocalin 2 is a regulator of macrophage polarization and NF-κB/STAT3 pathway activation. *Mol Endocrinol* 2014;28:1616–1628.
47. Parmar T, Parmar VM, Perusek L, Georges A, Takahashi M, Crabb JW, *et al*. Lipocalin 2 plays an important role in regulating inflammation in retinal degeneration. *J Immunol* 2018;200: 3128–3141.
48. Yang J, Moses MA. Lipocalin 2: a multifaceted modulator of human cancer. *Cell Cycle* 2009;8:2347–2352.
49. Sun B, Guo W, Hu S, Yao F, Yu K, Xing J, *et al*. Gprc5a-knockout mouse lung epithelial cells predicts ceruloplasmin, lipocalin 2 and periostin as potential biomarkers at early stages of lung tumorigenesis. *Oncotarget* 2017;8:13532–13544.
50. Hydbring P, De Petris L, Zhang Y, Brandén E, Koyi H, Novak M, *et al*. Exosomal RNA-profiling of pleural effusions identifies adenocarcinoma patients through elevated miR-200 and LCN2 expression. *Lung Cancer* 2018;124:45–52.